Unified model of nuclear mass and level density formulas

H. Nakamura
Nishi-Turuma 8-5-15, Yamato-city, Kanagawa-ken 242-0005, Japan

T. Fukahori
Japan Atomic Energy Research Institute, Tokai-mura, Ibaragi-ken 319-1195, Japan
(Received 25 February 2005; published 30 December 2005)

Nuclear ground and excited state properties are described by using parameter systematics on mass and level density formulas. The formulas are based on an analytical expression of the single-particle state density by introducing the shell-pairing correlation in a new way. Main features are the shell, pairing, and deformation effects on the droplet model near the ground state, which are washed out at higher excitation energies. The main aim of the paper is to provide in the analytical framework the improved energy dependent shell, pairing, and deformation corrections generalized to the collective enhancement factors, which offer a systematic prescription over a great number of nuclear reactions. The new formulas are shown to be in close agreement with not only the empirical nuclear mass data but also the measured slow neutron resonance spacings and experimental systematics observed in the excitation energy dependent properties.

DOI: 10.1103/PhysRevC.72.064329 PACS number(s): 21.10.Ma, 21.60.−n, 24.10.−i, 24.60.−k

I. INTRODUCTION

In recent years most statistical theory calculations of nuclear reactions have been carried out by using the semiempirical level density formula proposed by Gilbert and Cameron [1] in 1965, which is based essentially on the Fermi-gas (FG) model and seems to be enough to predict the level densities at a narrow range of excitations. However, it has in fact been well established [2] that the extrapolation of this formula to a wide range of excitation energies is subject to large errors, and that washing out shell effects should be considered. Among semiempirical models which account for the energy dependent shell correction of the nuclear level density, the model of Kataria, Ramamurthy, and Kapoor (KRK) [3] is considered the typical one. On the other hand, the energy dependent pairing corrections with the shell-pairing correlation seems to be only correctly considered by means of the microscopic Fermi-gas model [4] or of the extended Thomas-Fermi plus Strutinsky integral model [5], which based on the BCS theory of superconductivity still has, however, an inaccuracy due to the formalism in the superconducting phase [2,5].

The systematics of nuclear level density (LD) depends strongly on the shell, pairing, and deformation effects. The nuclear mass formula has been used to determine those "empirical" correction energies at the ground state, which are defined as corrections on the liquid-drop part in the mass formula. The most often used correction energies are those of Myers and Swiatecki (MS) [6], but discrepancies in absolute values between the measured and predicted masses may amount up to 2 MeV.

The main aim of the present work is to find a new set of parameter systematics for both the mass and the LD formulas on the basis of a new single-particle state density model. In this model, an analytical expression similar to the previous KRK model is adopted for the single-particle states, but the shell-pairing correlation terms are introduced in a new way [7], so this model is called the shell-pairing correlation (SPC) model.

We take the finite range droplet model (FRDM) [8], which is a new version of the previous MS model, as a starting point for the more detailed description of microscopic corrections, the shell, pairing, and deformation effects, based on the single-particle model.

In the next section, the formulas for energy- and spin-dependent properties of nuclei are presented. In Secs. III, IV, and V, the systematics of parameters for the ground state (mass formula) and for the excited state (LD formula) are obtained, and in Sec. VI the predictions of the current model are compared with those of the FG and KRK models by means of the empirical evaporation process data. The last section is the concluding remarks.

II. NUCLEAR STATISTICAL PROPERTIES

In the framework of the nuclear statistical model [1], thermodynamical properties are described by means of the grand partition function $\Omega(\lambda, \beta)$,

$$\Omega(\lambda,\beta) = \int g(\varepsilon)\ln[1+2\exp\beta(\lambda-\varepsilon)+\exp 2\beta(\lambda-\varepsilon)]d\varepsilon$$
$$= 2\int g(\varepsilon)\ln[1+\exp\beta(\lambda-\varepsilon)]d\varepsilon. \quad (1)$$

For a distribution function $g(\varepsilon)$ of the equidistant single-particle state, and the chemical potential λ assumed not to deviate appreciably from the Fermi energy, the following well-known relations for the entropy S and the excitation energy E^* are obtained:

$$S = 2a_0 t, \quad U = a_0 t^2, \quad a_0 = \frac{\pi^2}{3} g_0,$$
$$U = E^* - P_{\mathrm{oe}}, \quad P_{\mathrm{oe}} = n\Delta_0, \quad (2)$$

where a_0 is the asymptotic level density parameter, $t(=1/\beta)$ the thermodynamic temperature, g_0 the average density of

single-particle states (two-fold degenerate), U the effective excitation energy is defined by using $P_{\rm oe}$, which is the odd-even effect in the experimental pairing energy, $n = 0, 1, 2$ for odd-odd, odd, and even-even nucleus, Δ_0 the pairing energy gap at the ground state. The relations (2) are called the Fermi-gas (FG) model.

For more realistic analyses the distribution function $g(\varepsilon)$ in Eq. (1) is written in terms of the anisotropic harmonic oscillator model for the single-particle state density, considering only fundamental harmonics for the main shell with the subshell associated with the pairing interaction [7]:

$$\begin{aligned} g(\varepsilon) &= \sum_X g_{0X}\left[1 + \frac{1}{3} f_X \sum_i \cos\omega_{iX}(\varepsilon - \varepsilon_X)\right] \\ &\quad \times [1 - \cos\omega_{P_X}(\varepsilon - \lambda_X)], \\ \omega_{1X} &= \omega_{2X} = \omega_{\perp X} \approx \overline{\omega}\left(1 + \frac{1}{3}\delta_X\right), \\ \omega_{3X} &= \omega_{||X} \approx \overline{\omega}\left(1 - \frac{2}{3}\delta_X\right), \end{aligned} \tag{3}$$

δ_X quadrupole deformation parameter,

$\omega_{\rm PX}$ frequency related with the subshell spacing,

where the subscript x stands for the proton or neutron shell, f_X is the amplitude of the main shell, $\overline{\omega}$ is the average harmonic oscillator frequency related with the main shell spacing $\hbar\omega_{\rm sh}$, $\overline{\omega} = 2\pi/\hbar\omega_{\rm sh}$, $\hbar\omega_{\rm sh} = 41/A^{1/3}$, A is the mass number, $\varepsilon_X$is the main shell position, λ_X is the Fermi level for the x shell.

When $f_X = 0$ in Eq. (3), the so-called quasiparticle state density under the pairing correlation is written for an even-particle system

$$g(\varepsilon) = g_0[1 - \cos\omega_P(\varepsilon - \lambda)] \tag{4}$$

which is a prescription of the current model for pairing correlations.

A better understanding of the distribution function (4) can be obtained if the statistical properties of the quasiparticle system are expressed by using the traditional method of statistical mechanics. The main quantities are the excitation energy $U = E^*$ for an even-particle system, the entropy S, and the moment of inertia $\Im$:

$$\begin{aligned} U(t) &= a_0 t^2 - E_{P0}\{h_1(T_P)h_2(T_P) - 1\}, \\ S(t) &= 2a_0 t - t^{-1} E_{P0} h_1(T_P)\{h_2(T_P) - 1\}, \\ \Im(t) &= \Im_R h_3(T_P), \qquad T_P = \pi\omega_P t, \end{aligned} \tag{5}$$

where the functions $h_1(T_P)$ and $h_2(T_P)$ are defined as

$$\begin{aligned} &h_1(T) = T\,\mathrm{cosech}(T), \quad h_2(T) = T\coth(T) \\ &h_3(T) = \{1 - h_1(T)\}, \quad h_1(0) = 1, \\ &h_1(\infty) = 0, \quad h_2(0) = 1, \quad h_1(\infty)h_2(\infty) = 0, \end{aligned} \tag{6}$$

the symbol ∞ represents the asymptotic limit of high temperatures. The pairing energy at the ground state E_{P0} is defined as

$$E_{P0} = \sum_X g_{0x}/\omega_{\rm PX}^2. \tag{7}$$

If the empirical pairing energies are given, the frequency ω_p is determined by using Eq. (7).

The main features of the current prescription of Eq. (5) for pairing correlations can be compared with those of the simple version [5] of the BCS superconductivity theory, where for the energy gap at the ground state Δ_0 and for the temperature dependence of the gap parameter $\Delta(t)$ the following simple approximations are written as, for even nuclei,

$$\begin{aligned} 2\Delta_0/t_C &= 3.50, \\ \Delta(t) &= \Delta_0\left[1 - \left(\frac{t}{t_c}\right)^{3.23}\right]^{1/2} \qquad (t \leqslant t_C), \\ \Delta(t) &= 0.0 \qquad\qquad\qquad\qquad (t > t_C), \\ U &= a_0 t^2 + \frac{1}{2} g_0\left(\Delta_0^2 - \Delta^2\right), \\ S &= 2a_0 t F(\Delta/t)\omega_F(\Delta/t), \\ F(x) &= \frac{1}{\ln 2}\left[\ln(1 + e^{-x}) + \frac{x}{1 + e^x}\right], \\ \omega_F(x) &= 1 + 0.083x(1 - e^{-0.5x}), \\ \Im(t) &= \Im_R \mathrm{sech}^2\left(\frac{\Delta}{2t}\right), \qquad \Im_R = 0.015A^{5/3}, \end{aligned} \tag{8, 9}$$

where t_c is a critical temperature of the phase transition.

From Eqs. (5), (7), and (8), the following relations are assumed for the present model:

$$\begin{aligned} E_{P0} &= g_0/\omega_P^2 = \tfrac{1}{2} g_0 \Delta_0^2, \quad \omega_P = 2/\Delta_0, \\ \Delta &= \Delta_0\{h_1(T_P)h_2(T_P)\}^{1/2}. \end{aligned} \tag{10}$$

Figures 1 and 2 show plots of quantities, Δ, E_{p0}, S, and U of Eqs. (5) and (10) for the current SPC (shell-pairing correlation)

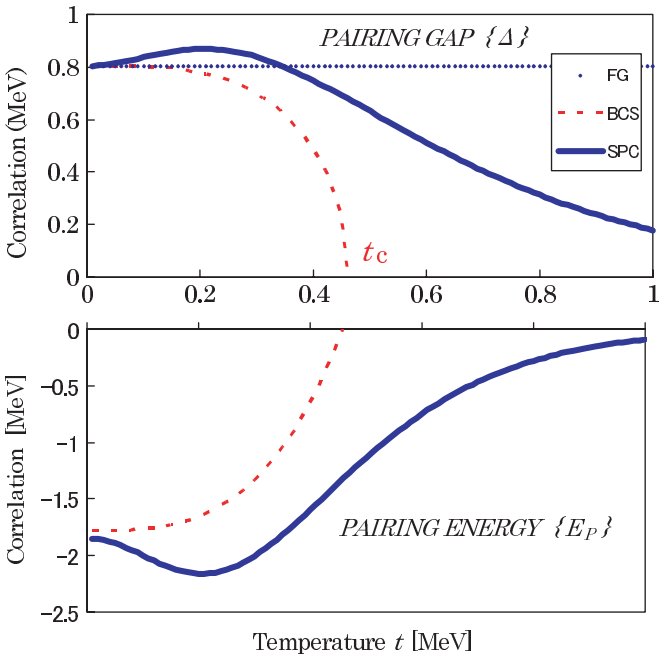

FIG. 1. (Color online) Plots of pairing correlations vs thermodynamic temperature for three different models of FG, BCS and SPC, as a sample of even-even nuclei. Values of parameter, $\Delta_o = 11/A^{1/2}$, $a_0 = 0.137A$, $A =$ mass number, $t_c = 2\Delta_0/3.50$, the critical temperature of phase transition in BCS model.

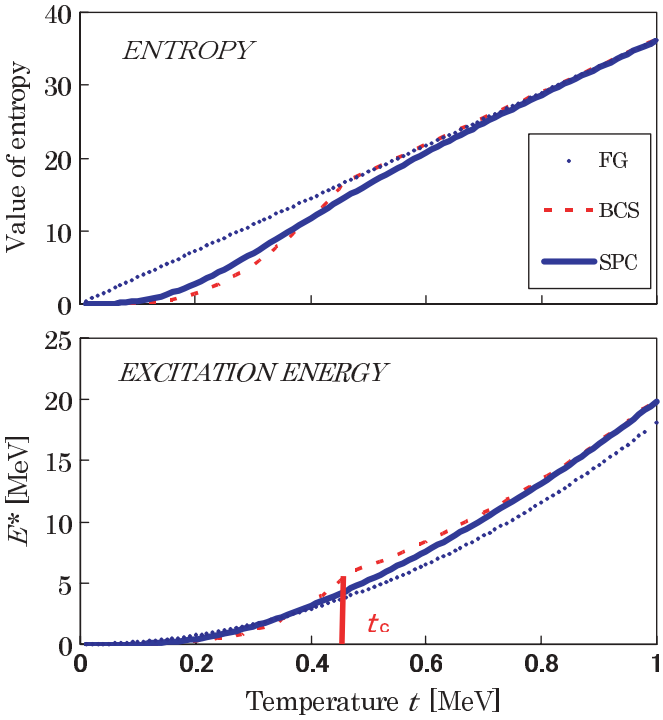

FIG. 2. (Color online) Plots of thermodynamic properties vs temperature for three different models of FG, BCS, and SPC, as a sample of paired even-even nuclei. (See also Fig. 1.)

model versus the thermodynamic temperature, compared with those of the FG, Eq. (2), and of the superconductor (BCS) model, Eq. (8). The following parameter systematics and its values are taken from the FG model estimate [2,6] as

$$a_0 = 0.137A, \quad \Delta_0 = 11/A^{1/2}. \tag{11}$$

The lack of an existence of the finite critical temperature of the phase transition in the current model is the prescription corresponding to the finite number of paired particles in the actual nucleus. Consequently, the discontinuous phase transition, known to be nonphysical for finite systems, is avoided by means of function (4).

In Eqs. (5) and (9) the moment of inertia $\Im$ tends to zero when the temperature vanishes. This approximation is inadequate to describe effects associated with the correlation between the pairing interaction and the rotational motion for deformed nuclei, and the following relation is reduced [9]:

$$\begin{aligned}
\Im_\perp &= \Im_R \left(1 + \frac{1}{3}\delta\right) h_\perp(\delta, \Delta), \\
h_\perp(\delta, \Delta) &= \left\{1 - d\left(\frac{41A^{1/3}\delta}{2\Delta}\right)\right\}, \\
\Im_3 &= \Im_R \left(1 - \frac{2}{3}\right) h_3(T_P), \\
d(x) &= \frac{\ln(x + \sqrt{1+x^2})}{x\sqrt{1+x^2}},
\end{aligned} \tag{12}$$

where $\Im_\perp$ is the perpendicular moment of inertia, $\Im_3$ the parallel moment of inertia is equal to that of Eq. (5).

By introducing the full scope of the single-particle state density of Eq. (3), $f_X \neq 0$, the statistical properties similar to Eq. (5) are written as

$$\begin{aligned}
S &= 2a_0 t + t^{-1} \sum_X [E_{S0X} h_1(T_{SX})\{h_2(T_{SX}) - 1\} \\
&\quad - E_{P0X} h_1(T_{PX})\{h_2(T_{PX}) - 1\}], \\
U &= a_0 t^2 + \sum_X [E_{S0X}\{h_1(T_{SX}) h_2(T_{SX}) - 1\} \\
&\quad - E_{P0X}\{h_1(T_{PX}) h_2(T_{PX}) - 1\}], \\
E_{S0X} &\equiv 2g_{0_X} \frac{1}{3} f_X \sum_i \omega_{Xi}{}^{-2} \cos 2\pi d_i \left(\chi_X - \frac{1}{2}\right), \\
E_{P0X} &\equiv 2g_{0_X} \omega_{PX}^{-2}\{1 + F_S(f_X, \chi_X, \delta_X)\} \\
&= \frac{1}{2}\overline{g}_X \Delta_{0X}^2, \\
F_S(f_X, \chi_X, \delta_X) &\equiv \frac{1}{3} f_X \sum_i \cos 2\pi d_i \left(\chi_X - \frac{1}{2}\right) \\
&\cong E_{s0x}(\overline{\omega}^2/2\overline{g}), \\
T_{SX} &= \pi\overline{\omega} t, \quad T_{PX} = \pi\omega_{PX} t, \\
\Im_3 &= \Im_R \sum_X \left(1 - \frac{2}{3}\delta_X\right) h_3(T_{PX}, T_{SX}), \\
\Im_\perp &= \Im_R \sum_X \left(1 + \frac{1}{3}\delta_X\right) h_\perp(\delta_X, \Delta_X), \\
h_3(T_{PX}, T_{SX}) &= [1 - h_1(T_{PX}) \\
&\quad - F_S(f_X, \chi_X, \delta_X)\{h_1(T_{SX}) - h_1(T_{PX})\}], \\
d_1 = d_2 &= \left(1 + \frac{1}{3}\delta_X\right), \quad d_3 = \left(1 - \frac{2}{3}\delta_X\right),
\end{aligned} \tag{13, 14}$$

where χ_X is the occupied fraction of the main shell, and E_{S0}, E_{P0} are the shell and pairing correction energies at the ground state. The fraction F_s on the right-hand side of E_{P0} describes the shell-pairing correlation effects.

III. SYSTEMATICS OF GROUND STATE PARAMETERS

In this section the ground state correction energies E_{S0} and E_{P0} in Eq. (14) are combined with the microscopic corrections, shell, pairing, and deformation terms of the nuclear mass formula, for which we can use, as a starting point, the macroscopic-microscopic approach of FRDM [8]. In the present model the nuclear mass (potential energy) can be written as

$$M(Z, N, \delta) = M_{\rm mac}(Z, N, 0) + M_{s+p}(Z, N, \delta), \tag{15}$$

where the ground-state nuclear mass $M(Z, N, \delta)$ is calculated as a function of proton number Z, neutron number N, and of shape parameter δ, and is the sum of a *spherical* macroscopic term $M_{\rm mac}$ and a *deformed* microscopic term M_{s+p}, representing the shell, pairing, and deformation corrections. As the spherical macroscopic term $M_{\rm mac}(Z, N, 0)$, including the Wigner term, we use those of FRDM, shown in Appendix A. Then, the deformed microscopic term $E_{s+p}(Z, N, \delta)$ can be

obtained from the experimental mass excess $M_{\rm exp}$,

$$S_{s+p}(Z,N,\delta) = M_{\rm exp}(Z,N) - M_{\rm mac}(Z,N,0) = S_Z + S_N, \tag{16}$$

where S_Z and S_N are the shell-group wise average (SGWA) corrections which include the shell, pairing, and deformation effects, and the basic assumption made in Eq. (16) is the independence of corrections due to the proton from those due to the neutron. The values of S_Z and S_N are obtained by means of the iteration procedure, each of which consists of two steps:

$$\begin{aligned} S_Z^{(i)} &= S_Z^{(i-1)} - \delta S_Z, \\ S_N^{(i)} &= S_N^{(i-1)} - \delta S_N, \\ \delta S_Z &= \sum_N W(Z)\{E_{\rm mac}(Z,N,0) + S_Z^{(i-1)} + S_N^{(i-1)} \\ &\quad - M_{\rm exp}\} \Big/ \sum_N W(Z), \\ \delta S_N &= \sum_Z W(N)\{E_{\rm mac}(Z,N,0) + S_Z^{(i-1)} + S_N^{(i-1)} \\ &\quad - M_{\rm exp}\} \Big/ \sum_Z W(N), \end{aligned} \tag{17}$$

$$\sigma_{\rm th} = \left[\frac{\sum_X {\rm W}(X)\{(M_{\rm th} - M_{\rm exp})^2 - \sigma_{\rm exp}(X)^2\}}{\sum_X {\rm W}(X)}\right]^{1/2}, \qquad W(X) = \frac{1}{\sigma_{\rm exp}^2(X) + \sigma_{\rm th}^2}, \tag{18}$$

where the theoretical error $\sigma_{\rm th}$ of Eq. (18) is defined as a measure of overall quality representing a precision that is constant in a certain range of computed masses $M_{\rm th} = E_{\rm mac} + S_Z + S_N$, e.g., for all experimental masses above $A = 16$, and its values are easily obtained in a few iterations. Each SGWA value of S_Z and S_N is obtained by averaging its value within a Z- or N-shell interval. Initial values of $S_Z^{(0)}$ and $S_N^{(0)}$ in Eq. (17) are estimated from the MS formula [6]. Final ones are obtained by requiring that the theoretical error $\sigma_{\rm th}$ should be a minimum when summed over all available experimental data. Through this work the experimental mass data of Ref. [10] are used, and the classification of mass data is shown in Table I. Also shown in Table I. (lower part) are results of error analyses for five different fitting models, MS, Möller *et al.*, ARA, SGWA and new mass formula, which are the polynomial fits to S_Z and S_N. In Fig. 3 the results of the above averaging procedure for S_Z and S_N are shown are (a) for the Z(I)-N(I) shell and (b) for the Z(I)-N(I+1) shell nuclei. Figure 4 shows components of microscopic corrections, by using the results shown in Fig. 3, for the new mass formula. The deformation energies reduced in Fig. 3 are used to estimate the values of deformation parameters δ shown in Fig. 5.

For obtaining new mass formula, polynomial fits to S_Z and S_N are made the following way:

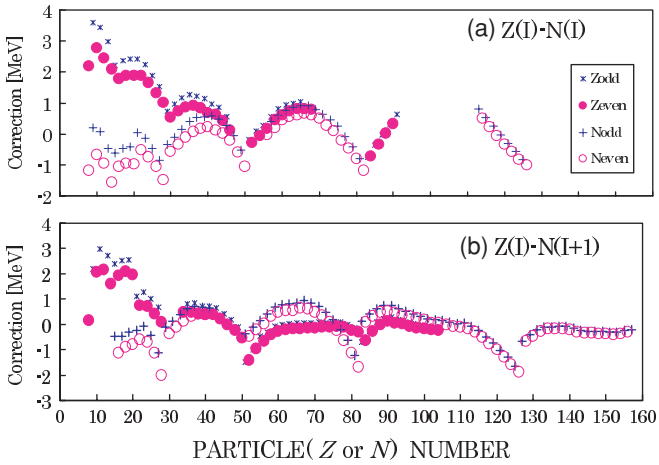

FIG. 3. (Color online) Microscopic corrections to FRDM based on Ref. [10] mass data. Values of corrections are derived by using the shellgroup wise average (SGWA) method, assuming the complete independence in interactions between proton and neutron shells on those corrections.

For even-particle nuclei:

$$\begin{aligned} S'_X(\chi_X) &\equiv C_{2X}{\chi_X}^2 + C_{1X}\chi_X + C_{0X}, \\ &\quad [C_{2X}, C_{1X}, C_{0X}]\text{: shell-structure parameters,} \\ S'_X &= \text{quadratic fits without the deformation defects,} \\ &\quad \{\text{Fig. 4 } \textit{Shell corrections } Z(I)\text{-}N(I+1)\ \textit{Shell}\} \\ S_X &= S'_X, \quad \text{for spherical nuclei,} \end{aligned} \tag{19}$$

$$\begin{aligned} E_{D0X} &= S'_X - S_X\text{: Deformation energy} \\ &\equiv D_{2X}{\chi_X}^2 + D_{1X}\chi_X + D_{0X}, \ \text{quadratic fits,} \\ &\quad [D_{2X}, D_{1X}, D_{0X}]\text{: deformation-effect parameters} \\ &= 0, \qquad \text{for spherical nuclei.} \end{aligned} \tag{20}$$

Values of deformation parameter δ_X:

$$\begin{aligned} E_{D0X} &= (2g_{0X})\omega^{-2} f_X F_d(\chi_X, \delta_X) \\ &= 1.44A^{1/3} f_X F_d(\chi_X, \delta_X), \\ F_d(\chi_X, \delta_X) &\equiv \frac{1}{3}\Sigma i\{di^{-2}\cos 2\pi(\chi_X - 1/2)di\} \\ &\quad - \cos 2\pi(\chi_X - 1/2) \\ d_1 = d_2 &= \left(1 + \frac{1}{3}\delta_X\right), \quad d_3 = \left(1 - \frac{2}{3}\delta_X\right). \end{aligned} \tag{21}$$

For odd-particle nuclei:

Pairing gaps (odd-even effects):

$$\begin{aligned} \Delta_{0X} &= \{(2/g_{0_X})E_{P0X}\}^{1/2} = (2/\omega_{\rm PX})[1 + F_S(f_X, \chi_X)]^{1/2}, \\ &\equiv C_{\rm PX}\{1 + C_{FX}S'_X(\chi_X)\}^{1/2} \\ &\quad [C_{\rm PX}, C_{FX}]\text{: pairing-effect parameters} \\ &\quad E_{P0X} = \tfrac{1}{2}g_X\Delta_{0X}^2\text{: pairing correlation energy.} \end{aligned} \tag{22}$$

The above mass formula parameters of shell structure, pairing, and deformation effects at the ground state are listed in Appendix B. The excitation energy dependences of those effects are described by using the energy dependences of

TABLE I. Microscopic corrections and fitting errors of mass formula.

Classification of measured mass excess (Ref. [10])								
Shell	N14	N20	N28	N50	N82	N126	N184	Total
Z14	46	34	8					88
Z20	8	35	35	7				85
Z28		7	54	53				114
Z50			6	192	267	2		467
Z82					179	418	9	606
Z126						62	232	294

Fitting error of nuclear mass formula [$\sigma_{\rm th}$(MeV)][d]

Shell		No. of Nuclei	MS[a]	Möller *et al.*[b]	Present model		
Z	N		(1967)	(1995)	ARA[c]	SGWA	New formula
14	14	46	7.125	0.856	0.716	0.569	0.736
	20	34	8.535	1.361	0.897	0.270	0.548
20	20	35	6.625	1.477	0.457	0.183	0.198
	28	35	9.202	1.362	0.511	0.119	0.230
28	28	54	6.529	1.146	0.485	0.392	0.413
	50	53	3.969	0.384	0.502	0.129	0.249
50	50	192	2.367	0.607	0.510	0.364	0.396
	82	267	1.331	0.709	0.640	0.331	0.455
82	82	179	1.115	0.483	0.606	0.500	0.569
	126	418	0.971	0.485	0.769	0.465	0.616
126	126	62	1.125	0.392	0.800	0.261	0.561
	184	232	1.301	0.392	0.535	0.450	0.614
Total		1607	3.165	0.662	0.659	0.409	0.535
Root mean squares (MeV)			3.179	0.674	0.678	0.409	0.551

Z14 shell: $Z = 8 \sim 14$, N20 shell: $N = 15 \sim 20$. Total = 1654 Nuclei.
Ranges of deformed nuclei: (Z28-N50, Z50-N82, Z82-N126, Z126-N184).
[a]Reference [6].
[b]Reference [8].
[c]ARA = all range average ($A = 16 \sim 263$).
[d]$\sigma_{\rm th}^2 = (1/\sum w_i)\sum w_i \lfloor (M_{\rm exp}^i - M_{\rm th}^i)^2 - {\sigma_{\rm exp}^i}^2 \rfloor$, $w_i = 1/({\sigma_{\rm exp}^i}^2 + \sigma_{\rm th}^2)^2$
$M_{\rm exp}^i$: measured mass, $M_{\rm th}^i$: estimated mass, $\sigma_{\rm exp}^i$: measured error.

Eqs. (6) and (13):

$$\begin{aligned} E_{\rm SX}(\chi_X) &= S'_X(\chi_X) H_{12}(T_{\rm SX}), \\ E_{\rm DX} &= E_{D0X} H_{12}(T_{\rm SX}), \\ E_{\rm PX} &= E_{P0X} H_{12}(T_{\rm PX}), \quad H_{12}(T) \equiv h_1(T) h_2(T), \end{aligned} \tag{23}$$

and shown in Fig. 6 as a sample of ^{238}U.

IV. NUCLEAR LEVEL DENSITIES

In the framework of the statistical model, the level density (LD) around the effective excitation energy U and spin J is written as [11–13]

$$\begin{aligned} \rho(U) &= \frac{\exp(S)}{2\pi\sqrt{D}}, \qquad D = \frac{18}{\pi^4} a^{1/2} U^{5/2}. \\ \rho(U, J) &= \frac{2J+1}{2\sqrt{2\pi}\sigma_{\rm eff}^3} \exp\left[-\frac{(J+1/2)^2}{2\sigma_{\rm eff}^2} \right] \rho(U) K_{\rm vib} K_{\rm rot}, \end{aligned} \tag{24}$$

where the collective enhancement factors, vibrational $K_{\rm vib}$ [5], and rotational $K_{\rm rot}$ [13] are defined as

$$\begin{aligned} K_{\rm vib} &= \exp(0.0555 A^{2/3} t^{4/3}), \quad K_{\rm rot} = \Im_\perp t, \quad (\delta_X > 0) \\ &\qquad\qquad\qquad\qquad = 1.0, \quad (\delta_X = 0) \\ \sigma_{\rm eff}^2 &= \Im_\perp^{2/3} \Im_3^{1/3} t, \end{aligned} \tag{25}$$

where the entropy S and the excitation energy U are described by Eq. (13),

$$\begin{aligned} S &= 2a_0 t + t^{-1} \sum_X \left[E_{S0X} h_1(T_{\rm SX}) \{ h_2(T_{\rm SX}) - 1 \} \right. \\ &\qquad \left. - E_{P0X} h_1(T_{\rm PX}) \{ h_2(T_{\rm PX}) - 1 \} \right], \\ U &= a_0 t^2 + \sum_X \left[E_{S0X} \{ h_1(T_{\rm SX}) h_2(T_{\rm SX}) - 1 \} \right. \\ &\qquad \left. - E_{P0X} \{ h_1(T_{\rm PX}) h_2(T_{\rm PX}) - 1 \} \right], \\ U &= E^* - \sum_X n_X \Delta_X \\ E_{S0X} &\equiv 2 g_{0_X} \frac{1}{3} f_X \sum_i {\omega_{Xi}}^{-2} \cos 2\pi d_i \left(\chi_X - \frac{1}{2} \right), \\ E_{P0X} &\equiv 2 g_{0_X} \omega_{\rm PX}^{-2} \{ 1 + F_S(f_X, \chi_X) \} = \frac{1}{2} g_{0_X} \Delta_{0X}^2. \end{aligned} \tag{26}$$

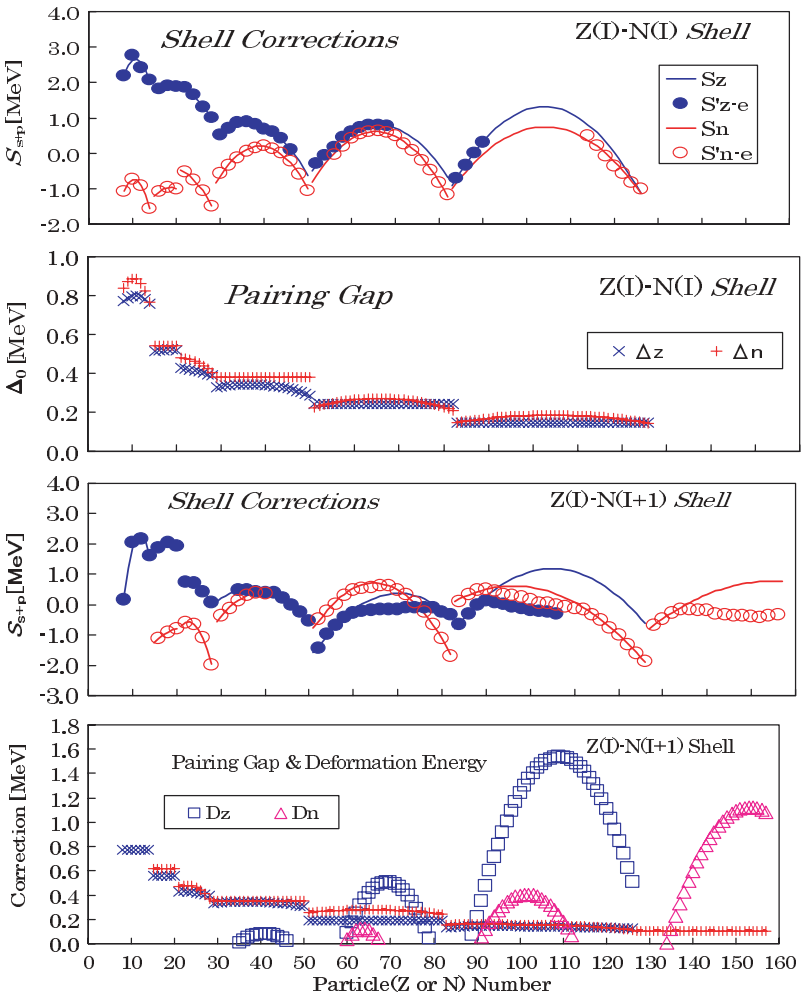

FIG. 4. (Color online) Polynomial expressions of correction energies, shell (—— proton, —— neutron), pairing (× proton, + neutron), and deformation (□ proton, △ neutron) of new mass formula. Symbols (● even-proton, ◯ even-neutron) are the SGWA values of microscopic correction energies for FRDM model.

In Eq. (26), $n_X = 0$, 1, for even-, odd-particle number, respectively.

The enhancement factors of Eq. (25) are plotted versus the excitation energy in Fig. 7, with the energy dependence of moment of inertias in the upper part of the figure.

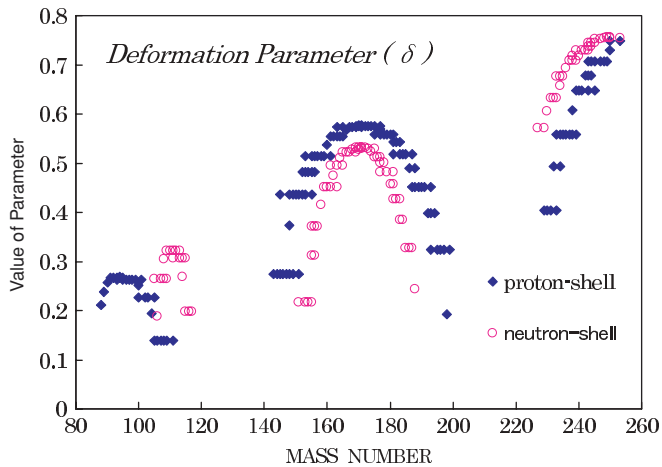

FIG. 5. (Color online) Values of ground state deformation parameter (δ), which are calculated by using Eq. (21).

V. SYSTEMATICS OF EXCITED STATE PARAMETERS

Free parameters to be fixed for excited states are α and ω_0 from Eqs. (2) and (3):

$$a_0 = \alpha A, \quad \overline{\omega} = \omega_0 A^{1/3}, \quad A = \text{mass number}. \tag{27}$$

where the values of α and ω_0 are the mass independent constants. A set of values (α, ω_0) for the relatively narrow mass range ($A = 41 \sim 67$) was determined for each of the typical LD formulas to fit s-wave neutron and proton average resonance spacings [2]. In the present work the neutron resonance

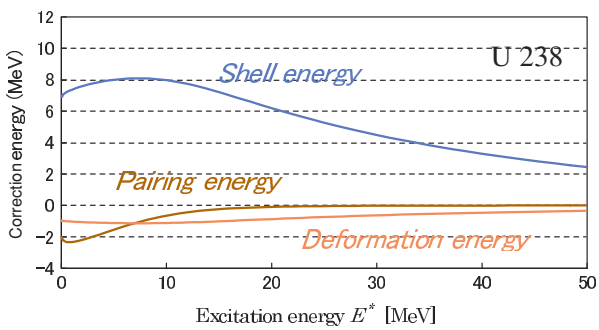

FIG. 6. (Color online) Excitation energy dependence of the microscopic corrections. [Eqs. (23)].

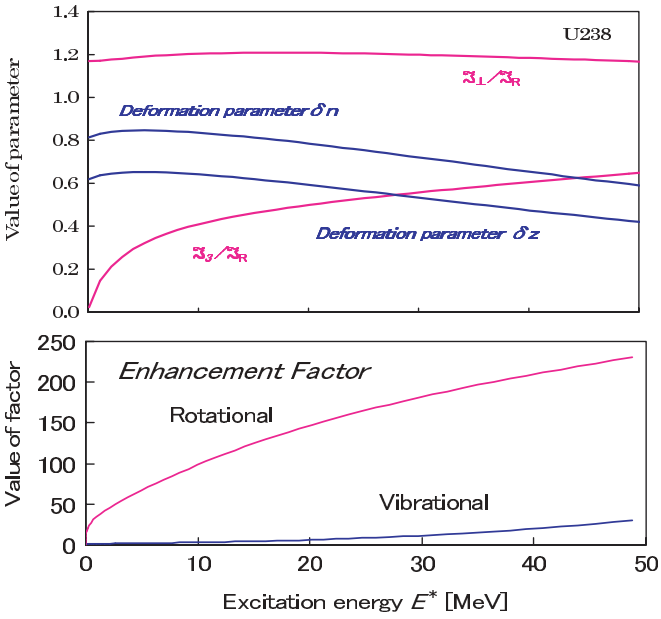

FIG. 7. (Color online) Plots of the moments of inertia and enhancement factors vs the excitation energy for ^{238}U nucleus, [Eqs. (25)]. $\Im_\perp$ is the perpendicular moment of inertia, $\Im_3$ the parallel moment of inertia, $\Im_R$ the rigid-body moment of inertia.

spacings for the wide range ($A = 24 \sim 253$) including deformed nuclei in Ref. [14] are used.

For the s-wave neutron resonance spacings $\langle D \rangle$ obs we obtain the following relations from Eqs. (24):

$$\begin{aligned}
&\rho(U, J) \equiv \rho(U, J : a_0),\\
&\rho(U, J = 1/2 : a_0) = 2/\langle D\rangle \text{ obs}, \quad \text{target spin } s = 0,\\
&\rho(U, s^{+1/2} : a_0) + \rho(U, s^{-1/2} : a_0) = 2/\langle D\rangle \text{obs}, \quad s \neq 0
\end{aligned} \tag{28}$$

which we used to extract values of the LD parameter a_0. Systematics of (α_0, ω_0) for three different models, FG, KRK, and SPC, are shown in Fig. 8. The constants α_0 and ω_0 are found by minimizing the quantity

$$\chi^2 = \sum_i (a_{0i} - \alpha_0 A_i)^2, \tag{29}$$

where the subscript i refers to the individual nuclei. The results of the linear least-squares fits for three models are shown in Table II. Those results give the slopes of curves of the neutron evaporation spectra due to three different models, and are used to verify its propriety by means of existing experimental evaporation spectra. The lower value of χ^2 means that its model gives a better average value of neutron s-wave resonance spacings than other models.

VI. COMPARISON OF PREDICTIONS BY DIFFERENT MODELS WITH EXPERIMENTAL EXCITATION PROPERTIES

Unlike the neutron resonance data, which are used for obtaining empirical systematics of LD parameters, in this

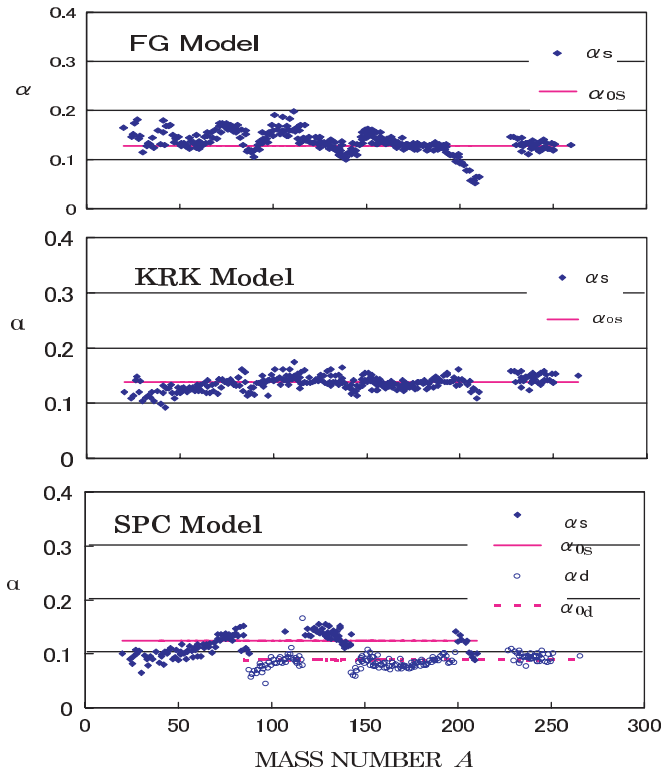

FIG. 8. (Color online) Systematics of level density parameter α, based on Ref. [14] resonance spacings data and on three different level density models, FG, KRK, and SPC.

section the data obtained both at low and high excitation energies E^* are involved. We obtained level densities from (a) counting low-lying bound levels at the energies [14], (b) level spacing data from several reactions (γ, p), (p, γ), (p, p'),(p, α), (α, γ), (α, n), (d, p), (^{3}He, d) (^{3}He, α) and the Ericson fluctuation measurements [15], and also (c) evaporation neutron spectra [16–20]:

(a): the cumulative levels $N(E^*)$ and the observable LD $\rho_{\text{obs}}(E^*)$ can give a good fit to the experimental data,

$$\begin{aligned}
N(E^*) &= \exp\{(E^* - U_O)/T\},\\
\rho_{\text{obs}}(E^*) &= (1/T)\exp\{(E^* - U_O)/T\},\\
&\quad T \text{ constant nuclear temperature},\\
&\quad U_0 \text{ backshift energy}.
\end{aligned} \tag{30}$$

TABLE II. Mass dependence of level density parameters (ω, α). Systematics are based on (Ref. [14]) data for the s-wave neutron resonances: $\overline{\omega} = \omega_0 A^{1/3}$, $a_S = \overline{\alpha}_S A$, $a_D = \overline{\alpha}_D A$, $\chi^2 = \sum_i (a_i - \overline{\alpha} A_i)^2$. The constants $(\omega_0, \overline{\alpha})$ are found by minimizing the quantity χ^2, where the subscript (i) refers to the individual nuclei, mass number A_i.

LD Model	$\omega_0 = \overline{\omega}/A^{1/3}$	$\overline{\alpha_S} = a_S/A$	$\overline{\alpha}_D = a_D/A$	χ^2
FG	—	0.128 ± 0.016	—	2809.6
KRK	0.181	0.139 ± 0.009	—	717.3
SPC	0.132	0.125 ± 0.012	0.088 ± 0.011	1011.3

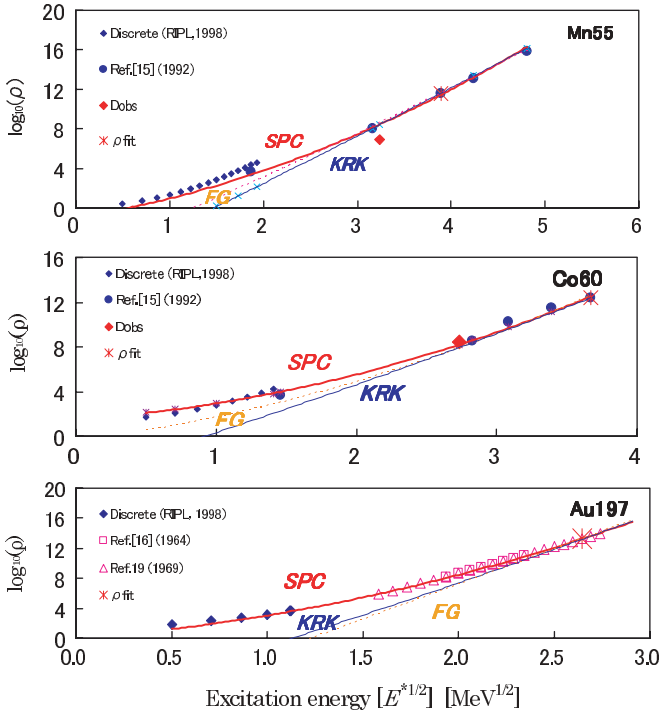

FIG. 9. (Color online) Plots of LD vs the excitation energy of the medium and heavy nuclei. Smooth curves are polynomial fittings to those values of three different models, using the LD parameter systematics in Table II.. D_{obs} corresponds to the average s-wave neutron resonance width and ρ_{obs} is a fixed point for all polynomial fitting curves.

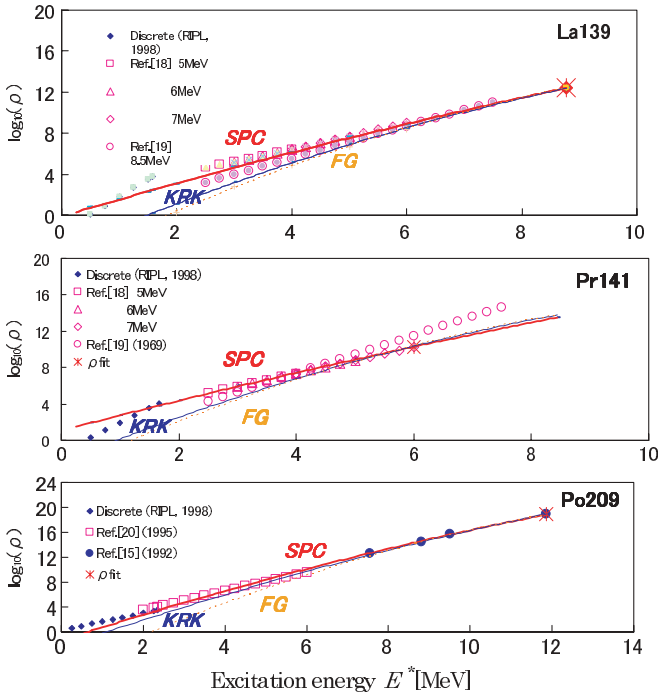

FIG. 10. (Color online) Plots of LD vs the excitation energy of closed-shell nuclei. See caption of Fig. 9.

(b): the observable LD $\rho_{obs}(U)$ is connected with the total density $\rho(U)$ by

$$\rho_{obs}(U) = \sum_J \rho(U, J) \approx \frac{\rho(U)}{\sqrt{2\pi}\sigma}. \tag{31}$$

(c): the relative intensity distribution $N(U)$ of evaporation neutron spectra can be written as [16]

$$\begin{aligned} N(E) &= \text{const.} E\sigma_c(E)\rho(U) \\ &= \text{const.} E\sigma_c(E)U^{-2}\exp\{2\sqrt{aU}\}, \end{aligned} \tag{32}$$

where E is the evaporated neutron energy, $\sigma_c(E)$ the compound formation cross section. The plots of the left-hand side of Eq. (32) versus $(E^*)^{1/2}$ or E^* test the LD formula

$$\begin{aligned} \log[N(E)U^2/E\sigma_c(E)] &= \sqrt{aU} + \text{const.}, \\ &\text{or} \\ &= U/T + \text{const.} \end{aligned} \tag{33}$$

the above is called the "slope technique" for testing the linearity of the right-hand side of Eq. (33).

For the first two cases, (a), (b), the absolute values of $\rho_{obs}(U)$ must be compared with predictions by each model of the LD, on the other hand, for the last case (c) only its slope is meaningful. Experimental LD data are classified into three different groups based on its excitation properties: Fig. 9 typical FG-gas type spectra of middle- and heavy-weight nuclei, Fig. 10 constant-temperature type of the closed-shell nuclei, Fig. 11 lower-slope (lower value of a) FG-gas type of deformed nuclei.

For the comparison of energy dependent LD of the present model (SPC) with those of FG and KRK models, a point on all curves, which are polynomial fittings to values of three

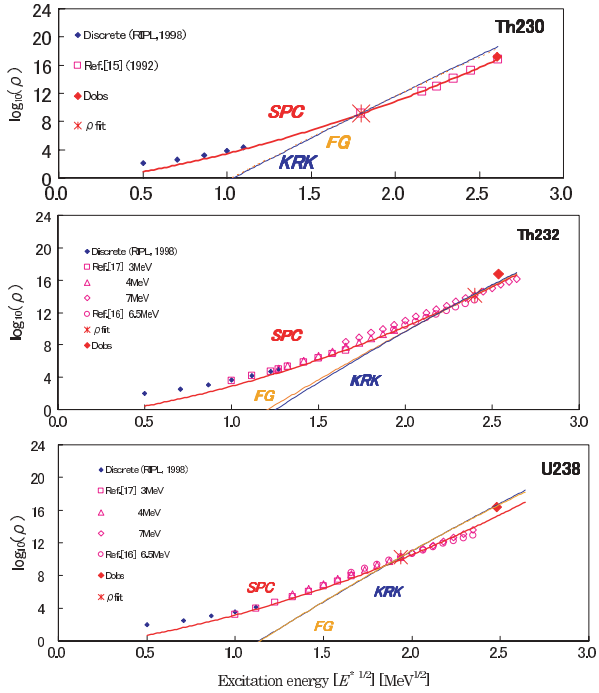

FIG. 11. (Color online) Plots of LD vs the excitation energy of deformed nuclei. See the caption of Fig. 9.

different models, is fitted as follows:

$$\log[\text{const.}\rho_{\text{obs}}(U)] = \log\{\rho_{\text{obs}}(U)\} + \text{const.} \quad (34)$$

on Figs. 9–11, where the LD parameters in Table II. are used for those models, and the collective enhancement factors, K_{vib} and K_{rot}, are not applied to FG and KRK models. The above normalization point for each nucleus is set for all polynomial fitting curves of three different models. Only the slopes are meaningful in the evaporation calculations, a point is selected, at first, for a curve of the SPC model to properly fit the experimental evaporation spectra, then, curves of other models are drawn to fit this point in turn.

These results show that the present LD model (SPC) is superior to other models.

VII. CONCLUSION

The semiempirical nuclear mass and LD formulas with the new parameter systematics are presented for the statistical theory analysis of a large number of nuclear reactions. The results of this work can be summarized as follows:

(i) The advantage of the present LD formula compared with the previous ones is its analytic form is consistent with all corrections and thus there is no use for separate tables of the shell, pairing, and deformation energies.

(ii) The present mass formula gives the improvements of accuracy in the shell, pairing, and deformation corrections compared with previous mass formulas, and the theoretical error over existing experimental masses ($A \geqslant 16$) is improved compared with those of Möller *et al.* [8] in Table I..

(iii) The *s*-wave neutron resonance spacing data for the mass range $A = 24$–253 including deformed nuclei were used to obtain the simple linear relations between the asymptotic level density parameter and the mass number, $a_0 = \alpha A$, for the spherical and deformed nuclei separately.

(iv) The results of analyses with data from counting low-lying bound levels and from using existing evaporation spectra show that the preferable predictions of weaker energy dependence by the present LD model compared with those the previous models, FG, KRK are due to the energy dependence of shell and pairing corrections, and also to the collective enhancement factors, in particular, the rotational ones for deformed nuclei.

ACKNOWLEDGMENTS

The authors would like to thank the members of the Working Group on parameters for theoretical calculations in the Japanese Nuclear Data Committee for their many comments on this work.

APPENDIX A: CONSTANTS OF THE FINITE RANGE DROPLET MODEL (FRDM)

Fundamental constants:

$M_H = 7.289034\,\text{MeV}$	hydrogen-atom mass excess
$M_n = 8.071431\,\text{MeV}$	neutron mass excess
$e^2 = 1.43997\,\text{MeV fm}$	electronic charge squared

Constants that have been determined from considerations other than nuclear masses:

$a_{\text{el}} = 1.433 \times 10^{-5}\,\text{MeV}$	electronic-binding constant
$K = 240\,\text{MeV}$	nuclear compressibility constant
$r_p = 0.80\,\text{fm}$	proton root-mean-square radius
$r_0 = 1.16\,\text{fm}$	nuclear-radius constant
$a = 0.68\,\text{fm}$	range of Yukawa-plus-exponential potential
$a_{\text{den}} = 0.70\,\text{fm}$	range of Yukawa function used to generate nuclear charge distribution

Constant obtained from consideration of mass-like quantities*:

$$W = 30\,\text{MeV}, \quad \text{Wigner energy} = W\left[|(N-Z)/A| + \begin{cases} 1/A, & (Z = N = \text{odd}) \\ 0, & (\text{otherwise}) \end{cases}\right]$$

Constants to be determined in a least-squares minimization:

$a_1 = 16.247\,\text{MeV}$	volume-energy constant
$a_2 = 22.92\,\text{MeV}$	surface-energy constant
$J = 32.73\,\text{MeV}$	symmetry-energy constant
$Q = 29.21\,\text{MeV}$	effective surface-stiffness constant
$c_a = 0.436\,\text{MeV}$	charge-asymmetry constant
$C = 60\,\text{MeV}$	preexponential compressibility-term constant.
$\gamma = 0.831$	exponential compressibility-term range constant

(*) pairing energies are included in the microscopic corrections.

APPENDIX B: POLYNOMIAL COEFFICIENTS FOR MICROSCOPIC CORRECTION TERMS

Shell-model Corrections: $S_0(\chi) = C_0 + C_1\chi + C_2\chi^2$.

Shell		*Z*-shell correction			*N*-shell correction		
Z	N	C_0	C_1	C_2	C_0	C_1	C_2
14	14	2.234	1.896	−2.107	−1.077	1.770	−2.249
	20	0.225	6.837	−5.504	−1.435	1.100	−0.456
20	20	1.613	0.812	−0.539	−1.356	1.045	−0.683
	28	1.398	1.851	−1.308	−0.923	2.156	−3.204
28	28	2.080	−0.721	−0.352	−0.435	−0.161	−0.888
	50	0.707	0.560	−1.192	−0.752	4.495	−4.403
50	50	0.319	2.930	−3.884	−1.064	5.022	−4.959
	82	0.010	2.517	−3.070	−0.999	7.417	−8.045
82	82	−0.673	5.947	−5.955	−1.023	6.738	−6.951
	126	−1.795	6.929	−5.519	−0.040	3.558	−5.511
126	126	−1.134	9.777	−9.780	−1.171	7.609	−7.556
	184	−0.992	8.370	−8.014	−0.893	−6.702	−6.703

Deformation energy: $E_{D0}(\chi) = D_0 + D_1\chi + D_2\chi^2$.

Shell		Z-shell correction			N-shell correction		
Z	N	D_0	D_1	D_2	D_0	D_1	D_2
50	82	−0.286	1.264	−1.080	−1.116	5.884	6.949
82	126	−1.308	6.041	−5.022	−0.798	5.422	6.088
126	184	−1.124	8.632	−6.996	−1.119	9.571	10.166

Pairing energy-gap: $\Delta_0(\chi) = C_p\{1 + C_F S_0(\chi)\}^{1/2}$.

Shell		Z-shell paring		N-shell pairing	
Z	N	C_p	C_F	C_p	C_F
14	14	0.619	0.250	0.982	0.250
	20	0.775	0.000	0.617	0.000
20	20	0.429	0.025	0.541	0.000
	28	0.556	0.000	0.517	0.250
28	28	0.349	0.250	0.511	0.250
	50	0.394	0.245	0.353	0.000
50	50	0.312	0.250	0.379	0.000
	82	0.328	0.250	0.268	0.115
82	82	0.245	0.000	0.253	0.250
	126	0.194	0.020	0.153	0.250
126	126	0.150	0.000	0.170	0.250
	184	0.000	0.000	0.105	0.000

[1] A. Gilbert and A. G. W. Cameron, Can. J. Phys. **43**, 1446 (1965).
[2] H. Vonach, M. Uhl, B. Strohmaier, B. W. Smith, E. G. Bilpuch, and G. E. Mitchell, Phys. Rev. C **38**, 2541 (1988).
[3] S. K. Kataria, V. S. Ramamurthy, and S. S. Kapoor, Phys. Rev. C **18**, 549 (1978).
[4] L. G. Moretto, Nucl. Phys. **A182**, 641 (1972).
[5] S. Goriely, Nucl. Phys. **A605**, 28 (1996).
[6] W. D. Myers and W. J. Swiatecki, Nucl. Phys. **81**, 1 (1966); Ark. Fys. **36**, 343 (1967).
[7] H. Nakamura, IAEA report, INDC(JPN)-172/U, 1994.
[8] P. Möller, J. R. Nix, W. D. Myers, and W. J. Swiatecki, At. Data Nucl. Data Tables **59**, 185 (1995).
[9] A. B. Migdal, Nucl. Phys. **13**, 655 (1959).
[10] G. Audi and A. H. Wapstra, Nucl. Phys. **A595**, 409 (1995).
[11] S. Bjornholm, A. Bohr, and B. Mottelson, *Proceedings of Conference on Physics and Chemistry of Fission* (IAEA, Vienna, 1974), Vol. 1, p. 367.
[12] A. Bohr and B. Mottelson, *Nuclear Structure* (Benjamin, New York, 1975), Vol. II.
[13] A. V. Ignatyuk, K. K. Istekov, and G. N. Smirenkin, Sov. J. Nucl. Phys. **29**, 450 (1979).
[14] Reference Input Parameter Library (RIPL) file, IAEA-TECDOC-1034, 1998.
[15] A. S. Iljinov, M. V. Mebel, N. Bianchi, E. De Sanctis, C. Guaraldo, V. Lucherini, V. Muccifora, E. Polli, A. R. Reolon, and P. Rossi, Nucl. Phys. **A543**, 517 (1992).
[16] S. G. Buccino, C. E. Hollandsworth, H. W. Lewis, and P. R. Bevington, Nucl. Phys. **60**, 17 (1964).
[17] R. Batchelor, W. B. Gillboy, and J. H. Towle, Nucl. Phys. **65**, 236 (1965).
[18] R. O. Owens and J. H. Towle, Nucl. Phys. **A112**, 337 (1968).
[19] M. Maruyama, Nucl. Phys. **A131**, 145 (1969).
[20] A. Wallner, B. Strohmaier, and H. Vonach, Phys. Rev. C **51**, 614 (1995).